

Shape of atomic steps on Si(111) under localized stressHiroo Omi,* David J. Bottomley, Yoshikazu Homma, and Toshio Ogino
*NTT Basic Research Laboratories, NTT Corporation, Atsugi, Kanagawa 243-0198, Japan*Stoyan Stoyanov and Vesselin Tonchev
Institute of Physical Chemistry, Bulgarian Academy of Sciences, 1113 Sofia, Bulgaria
(Received 24 May 2002; published 5 August 2002)

Localized elastic strain in Si crystal is artificially produced by buried silicon oxide inclusions formed beneath a lithographically defined area by oxygen implantation. The Si crystal with local strain is annealed at 1180–1260 °C, and the shape of atomic steps at a vicinal Si(111) surface is observed by *in situ* ultrahigh-vacuum secondary-electron microscopy and *ex situ* atomic force microscopy. The step shape is determined by the balance between the elastic stress at the surface and the Gibbs-Thomson effect—the decrease of the chemical potential μ related to the step curvature. The shape analysis enables us to estimate the strain-related contribution to the Gibbs free energy density $\Delta G/A = 8.3 \times 10^{-5} \text{ J/m}^2$.

DOI: 10.1103/PhysRevB.66.085303

PACS number(s): 68.35.Bs

I. INTRODUCTION

Atomic steps on a silicon surface have received much attention from scientific as well as technological viewpoints.¹ This is because atomic steps have great potential as templates for nanostructure self-assembly, which is promising for future nanoscale device fabrication.² To be able to control these nanostructures, such as quantum dots and wires, on the desired area of a Si wafer, it is crucial that we understand the nature of atomic steps on the Si surface.

Elastic strain or stress is one of the significant factors governing the shape of steps^{3–7} and step bunching.^{8,9} The effects of strain or stress on the steps have been clearly demonstrated on Si(001) under applied strain^{3,4} and on SiGe(001) under epitaxial strain on the wafer scale.⁵ The atomic steps naturally align themselves in order to relieve the strain effectively on surfaces, suggesting that they can be patterned by the strain on surfaces. For nanostructure applications, however, the degree and distribution of strain have to be engineered not only on the wafer scale, but also on the nanoscale level. In this context, we have very recently demonstrated surface strain distribution control on a Si surface by means of buried silicon oxide inclusions. The inclusions are formed beneath a lithographically defined area by oxygen implantation and subsequent high-temperature annealing.¹⁰ The formation of silicon oxide inclusions within the Si bulk produces strain at the surface because when silicon oxidizes its volume doubles. Our success in producing this novel surface has opened a new field: the physics of localized strain on Si surfaces. We have demonstrated that the strain distribution on Si(001) enables the growth of uniform Ge nanostructures with the desired spatial arrangement on a wafer scale.¹⁰

In addition to the control of steps, it is particularly important in surface physics to measure and quantify the silicon surface energy under localized strain. However, this has received little attention, to our knowledge, despite its importance for nanostructure self-assembly.

In this paper, we report on the shape of atomic steps on Si(111) under localized strain induced by buried silicon oxide inclusions. We show that the thermodynamics accounts

for the strain-driven equilibrium shape of monatomic steps on Si(111), and a step shape analysis yields the strain-related Gibbs free energy in a local strained area.

II. EXPERIMENT

First, a mask was made on Si(111) wafers miscut by 1.63° toward 7° from the $[11\bar{2}]$ direction (terrace width = 11.1 nm) and the mask was patterned using optical lithography to produce line shapes. The mask consists of an 800-nm-thick chemical vapor deposition (CVD) grown oxide on top of 100 nm of poly-Si. The poly-Si lies on top of a 100-nm-thick thermal oxide, which is on top of the Si wafer. Next, oxygen ions were implanted into the partially masked substrate at an energy of 180 keV and at an areal density of $2 \times 10^{17} \text{ cm}^{-2}$. Oxygen ions penetrated the Si substrate only where openings in the mask existed. The entire mask was etched off in a HF:H₂O (25%:75%) solution. The substrate was then annealed in an Ar atmosphere containing 0.2% O₂ at 1325 °C for 2.5 h. Silicon oxide inclusions were thereby formed at selected places within the Si bulk to create localized stress on the Si surface. Finally, the 50-nm-thick surface silicon oxide that grew during the 1325 °C anneal was chemically etched off in HF:H₂O (5%:95%) solution.

The shape of the steps and their distribution were observed with an *in situ* ultrahigh-vacuum secondary-electron microscope (UHV-SEM) at low magnification and with an *ex situ* atomic force microscope (AFM) at high magnification. In the SEM experiments, we annealed the sample at 1180 and 1230 °C under debunching and bunching conditions (both directions of the electric current) and also annealed a sample at 1260 °C for 15 s. The pressure during annealing was less than 2×10^{-9} Torr. Micro-Raman spectroscopy measurements were performed at a wavelength of 457 nm with a 1- μm -diam lateral resolution.

III. RESULTS AND DISCUSSION

Figure 1(a) shows the AFM image, obtained from Si(111) with silicon oxide inclusions beneath line areas formed by

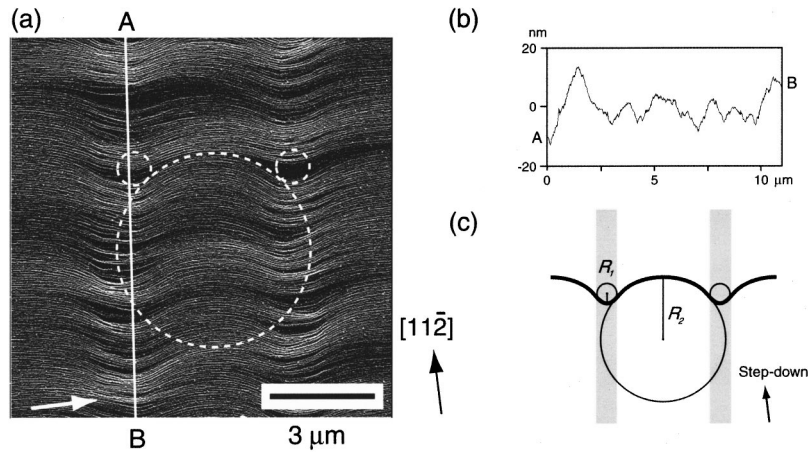


FIG. 1. (a) AFM image of Si(111) with buried silicon oxide inclusions for a pair of 700-nm-wide implantation line patterns after 1 min heating at 1230 °C with direct current in the step-down direction (debunching condition). The white arrow indicates the direction of direct current for the step-parallel heating. (b) Height profile along line A-B in (a). (c) Schematic illustration of an atomic step in (a) and of the definition of the step curvatures. Shaded areas in (c) are the areas where buried silicon oxide inclusions produce tensile strain.

implanting through 700-nm-wide line patterns, as illustrated in Figs. 1(c) and 2. White lines and black areas in Fig. 1(a) correspond to steps and terraces, respectively. Various characteristic features due to local strain were observed on the surface: a step and terrace structure was observed, indicating that the Si adatoms sublime from the surface in the step-flow mode by annealing at 1230 °C. Eighty percent of the steps on the implanted line regions were bunched; they did not bunch in the region between the two shaded areas. The average step height is 3.3 bilayers (BL) in the implanted line regions and 1.2 BL between the two line regions. The step bunching in the line regions is qualitatively consistent with the theory of stress-induced step bunching on vicinal surfaces by Tersoff *et al.*,⁸ indicating that the line regions are the more strained.¹⁰ In addition, the reduced step bunching in the region between the lines indicates that the region is at low strain. The surface on the strained lines has step bands composed of bunched steps. The height profile along the white line in Fig. 1(a) indicates that the height of the step bands is 13 nm on average, which corresponds to 41 BL [Fig. 1(b)]. Monatomic steps were observed on wide terraces between the step bands. Shape analysis of the monatomic steps is discussed below. In Fig. 1(b), the apparent step-down direction (from A to B) regions are in fact flat, approximately: the negative apparent gradient is due to the background subtraction employed in the data analysis. Both bunched and single monatomic steps on the surface curve concavely on the strongly strained areas and convexly in the low-strain

region during step-flow sublimation. The radius of curvature of a monatomic step in a bunch is 700 nm in the areas above the SiO₂ inclusions and 4100 nm in the low-strain area between the inclusions [Fig. 1(c)]. We also measured the radius of the curvature of a single monatomic step, situated in a large terrace between the bunches. The single step has a smaller radius of curvature $R_1 = 350$ nm.

The above step structure appeared at the Si(111) surface after annealing at 1230 °C for several seconds. After 2 min of further annealing, *in situ* SEM and *ex situ* AFM showed no further change in step shape. When we changed the electric current direction, we could not observe any significant change in step shape and step height distribution in the strained regions for step-down (step debunching), step-up (step bunching), and intermediate step-parallel current directions at 1230 °C. The typical length of the step band caused by dc current observed on the strain free region is consistent with the previous report by Homma and Aizawa.¹¹

To understand the physics behind the bell-like shape of the steps in Fig. 1(a) it is convenient to analyze the equilibrium shape of the monatomic steps, although the Si crystal in our experiment is heated to 1230 °C in UHV and considerable evaporation takes place. The shape of the steps is determined by two physical factors: the strain at the surface and the step free energy. The free energy of the concave step has a negative contribution to the local chemical potential μ and partially compensates the strain-related increase of μ . The equilibrium shape of the step is determined by the requirement that the local chemical potential have a constant value along the step. The step curvature changes μ by an amount $\Delta\mu$ such that $\Delta\mu(R_1) = -\Omega\gamma/R_1$ and $\Delta\mu(R_2) = \Omega\gamma/R_2$ [Figs. 1(a) and 1(c)], where Ω is the area per atom at the surface and γ is the step free energy per unit length.¹² Here R_1 is the radius of curvature of the monatomic step in the tensile strain area; R_2 is the corresponding quantity in the area of much weaker compressive strain [Fig. 1(c)] (R_1 and R_2 are both taken to be positive). In fact, the step stiffness should appear in the expression for $\Delta\mu$ instead of γ , but at the high temperatures used in the experiments the anisotropy of γ is small and the step stiffness is practically equal to the step free energy. The measurements show R_1 to be constant over a large fraction of the tensile strain area and R_2 to be

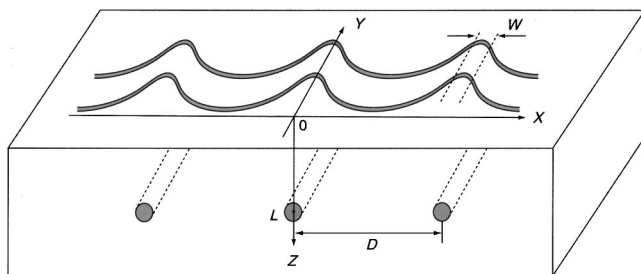


FIG. 2. Schematic illustration of steps on Si(111) with buried silicon oxide inclusions. Inclusions were formed at a depth of about 300 nm, as observed by cross-sectional transmission electron microscopy.

constant in a large fraction of the weak-compressive-strain area. This provides grounds to estimate the contributions $\Delta\mu(R_1)$ and $\Delta\mu(R_2)$ to the local chemical potential. The requirement for a constant chemical potential along the step [Fig. 1(c)] is

$$\Delta\mu_{1\text{str}} + \Delta\mu(R_1) = \Delta\mu_{2\text{str}} + \Delta\mu(R_2), \quad (1)$$

where $\Delta\mu_{1\text{str}}$ is the strain-related contribution to the chemical potential in the tensile strain area [the shaded areas in Fig. 1(c)] and $\Delta\mu_{2\text{str}}$ is the corresponding quantity in the area of weak compressive strain (the area around the middle point between two neighboring inclusions). Equation (1) can be rewritten in the form

$$\Delta\mu_{\text{str}} = \Omega\gamma\left(\frac{1}{R_1} + \frac{1}{R_2}\right), \quad (2)$$

where $\Delta\mu_{\text{str}} = \Delta\mu_{1\text{str}} - \Delta\mu_{2\text{str}}$. Since the chemical potential is equal to the Gibbs free energy per particle, it is convenient to write $\Delta\mu_{\text{str}} = (\Omega/A)\Delta G_{\text{str}}$, where ΔG_{str} is the difference between the strain-related contributions to the Gibbs free energy G in the tensile and weak-compressive-strain areas (G refers to an area A and, on the other hand, the contribution of the weak compressive strain is much smaller than the contribution of the strong tensile strain in the areas above the SiO_2 inclusions; i.e., ΔG_{str} is practically equal to the strain-related contribution to the Gibbs free energy). Therefore, Eq. (2) can be rewritten in the form

$$\frac{\Delta G_{\text{str}}}{A} = \gamma\left(\frac{1}{R_1} + \frac{1}{R_2}\right), \quad (3)$$

making it possible to estimate the surface density of the strain-related contribution to the Gibbs free energy by simply measuring the radii of curvature of the steps at the crystal surface.

Using the values $R_1 = 700$ nm and $R_2 = 4100$ nm, determined in our experiments for a step in a bunch, and the step free energy per unit length $\gamma = 0.5 \times 10^{-10}$ J/m,^{13,14} we obtain $\Delta G/A = 8.3 \times 10^{-5}$ J/m² for the surface density of the strain-related Gibbs free energy. Besides the above value of the step free energy, a substantially (2–3 orders of magnitude) larger value of γ has been determined from the interpretation of the experimental data on evaporation of Si(111) in the temperature interval 1050–1100 °C.¹⁵ Substituting this value of γ into Eq. (3), we obtain, for $\Delta G/A$, 2–3 orders of magnitude larger values than those given above.

As already mentioned, a small number of steps are not included in the bunches. These steps (situated at the large terraces between the step bunches) have a smaller radius of curvature in the area of strong tensile strain. For one of these steps we obtained $R_1 = 350$ nm and R_2 tending to infinity. Substituting these values into Eq. (3), we obtained $\Delta G/A = 1.4 \times 10^{-4}$ J/m² for $\gamma = 0.5 \times 10^{-10}$ J/m and 2–3 orders of magnitude larger values of $\Delta G/A$ when γ has the value estimated by Latyshev *et al.*¹⁵

Micro-Raman spectroscopy measurements of stress in a strained area, corrected slightly for the limited resolution,¹⁰ showed in the (111) plane a 17 ± 3 MPa difference in the

stress values between the tensile and compressive stress regions. This corresponds to a strain energy of 3.6×10^{-3} J/m² under a Gibbs free energy assumption and 4.0×10^{-7} J/m² under a Helmholtz assumption.¹⁶ These energies are overestimated by factors of about 6 for the Gibbs assumption and of about $6^2 = 36$ for the Helmholtz assumption due to the nonzero (about 140 nm) depth probed by the micro-Raman technique. After correction for the micro-Raman resolution, the energies derived from the step curvatures are consistent with the Gibbs free energy, but not with the Helmholtz free energy.

More detailed treatment of the shape $Y(X)$ of the steps (Fig. 2) should account for the variation of the strain at the surface. To derive a differential equation for $Y(X)$ we note that, mathematically, the curvature is given by the expression $R^{-1} = Y''(1 + Y'^2)^{-3/2}$ and the requirement for a constant value of the chemical potential along the step reads

$$\Omega\gamma\frac{Y''}{(1 + Y'^2)^{3/2}} + \Delta\mu_{\text{str}} = \text{const.} \quad (4)$$

To obtain an explicit form of the differential equation for $Y(X)$ we need an expression for $\Delta\mu_{\text{str}}$ as a function of the distance X (Fig. 2). Since our measurements manifest a constant curvature of the step in the vicinity of $X = 0$ (an indication of a constant strain energy density in this area), we introduce the parameter W , which is the width of the stripe, where the strain at the surface has a constant value. One should keep in mind, however, that, in fact, the “wires” consist of separate clusters [the cross-sectional transmission electron microscope (TEM) image of the “wire” typically shows about five inclusions of SiO_2], which leads to considerable variation of the parameter W . That is why the shape of the steps can vary considerably from place to place at the crystal surface. Outside the stripe (i.e., for $|X| > W/2$) the strain at the surface and the local chemical potential decrease. We assume for $|X| \geq W/2$,

$$\Delta\mu_{\text{str}}(X) = \frac{A'}{\left[L^2 + \left(|X| - \frac{W}{2}\right)^2\right]^{3/2}} \left[1 - \frac{3L^2}{L^2 + \left(|X| - \frac{W}{2}\right)^2}\right]^2, \quad (5)$$

where L is the distance from the center of the inclusion (from the axis of the “wire”) to the crystal surface and A' is a constant. [We take $A' = \Delta\mu_{\text{str}}^0 L^6/4$, where $\Delta\mu_{\text{str}}^0$ is the constant value of the strain-related chemical potential inside the stripe $|X| \leq W/2$ so that $\Delta\mu_{\text{str}}(X)$ is a continuous function at $X = \pm W/2$.] This expression for the decrease of $\Delta\mu_{\text{str}}$ with X is similar to the formula derived by Tersoff *et al.*¹⁷ (using an earlier work by Maradudin and Wallis¹⁸), which describes the dependence of the strain energy E_{el} on X to within a constant A' . The strain fields of neighboring “wires” of inclusions (the distance between neighboring “wires” is D) overlap so that the shape of the step is influenced by the strain energy induced by two neighboring “wires.” Introducing dimensionless coordinates $x = X/L$, $y = Y/L$ and dimensionless parameters $d = D/L$ and $w = W/L$, we can write (for $w/2 < x < d - w/2$)

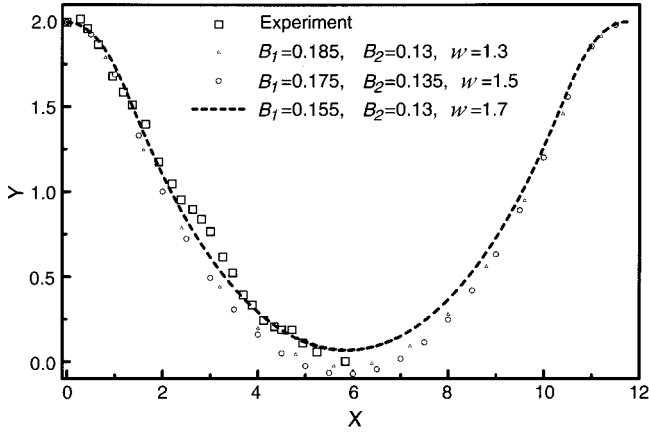


FIG. 3. Shape of a monatomic step on Si(111). Squares are data measured on a sample; all other curves are theoretically calculated step shapes [obtained by integrating Eqs. (4) and (6) with the values of B_1 , B_2 , and w listed in the figure].

$$\begin{aligned} \frac{y''}{(1+y'^2)^{3/2}} &= - \frac{B_1}{\left[1 + \left(d-x - \frac{w}{2}\right)^2\right]^{3/2}} \left[1 - \frac{3}{1 + \left(d-x - \frac{w}{2}\right)^2}\right]^2 \\ &\quad - \frac{B_1}{\left[1 + \left(x - \frac{w}{2}\right)^2\right]^{3/2}} \left[1 - \frac{3}{1 + \left(x - \frac{w}{2}\right)^2}\right]^2 + B_2. \end{aligned} \quad (6)$$

To obtain the shape of the step, we integrated the differential equations (4) and (6), using the initial condition $y'(0)=0$. Equation (4) with $\Delta\mu_{\text{str}} = \Delta\mu_{\text{str}}^0$ holds good inside the stripe $-w/2 < x < w/2$ where the strain at the surface has a constant value. [We have rewritten Eq. (4) in dimensionless coordinates $x=X/L$, $y=Y/L$ like in Eq. (6).] After integrating Eq. (4) in the interval $0 \leq x \leq w/2$, we switch to Eq. (6) in the interval $w/2 < x < d-w/2$ and, finally, we again integrate Eq. (4), this time in the interval $d-w/2 \leq x \leq d$. The constants B_1 , B_2 , and w are used as fitting parameters. On the other hand, the constant B_1 is given by the expression

$$B_1 = \frac{1}{\Omega \gamma} \frac{L}{4} \Delta\mu_{\text{str}}^0,$$

so that the value of $\Delta\mu_{\text{str}}^0$ can be estimated from it, which provides a reasonable fit of the theoretical curve to the shape of the steps in our experiments. Since $\Delta\mu_{\text{str}}^0 = (\Omega/A)\Delta G^0$, it is convenient to rewrite the last expression in the form $\Delta G^0/A = B_1 4 \gamma/L$ to allow an estimation of the surface density $\Delta G^0/A$ of the strain-related Gibbs free energy in the area $-w/2 < x < w/2$. Figure 3 shows the shape of a step obtained by integrating Eqs. (4) and (6) as explained above. There is relatively good agreement with the experimentally determined shape (presented by the squares) at $B_1 = 0.155$ (the

values of the other parameters are given in Fig. 3). Making use of these values of B_1 , $L = 330$ nm, and $\gamma = 0.5 \times 10^{-10}$ J/m,^{13,14} we estimated correspondingly $\Delta G^0/A = 9.3 \times 10^{-5}$ J/m² and $\Delta G^0/A = 7.8 \times 10^{-5}$ J/m² and found good agreement with the values obtained on the basis of Eq. (3) and the measured radii of curvature R_1 and R_2 .

The considerations outlined above have several weak points. The first one is related to the rather different values, reported by different authors for the free energy of the steps on Si(111) surfaces. This circumstance leads to rather different values of the strain-related Gibbs free energy which is estimated by multiplying the measured curvature of the steps and the step free energy [see Eq. (3)]. The problem is also related to the quenching of the samples. The point is that, according to Ref. 15, the step free energy substantially depends on the temperature in the interval 1230–1380 °C. Thus the question arises, could the shape of the steps change during the quenching because of the temperature-induced change of the step free energy? It is difficult to answer this question. This complication, however, could be avoided by using the “in real time” technique of observation like low-energy electron microscopy, for example.

Another problem is related to the fact that the steps in the strained area of the surface form bunches, which could, in principle at least, change the shape of the steps (because of the step-step interactions, for instance). One way out seems to be an analysis of the shape of the single steps, situated in the large terraces between the bunches. These steps, however, move rather fast: i.e., they are not under “near-to-equilibrium conditions” and their shape could be substantially influenced by kinetic factors. As pointed out above, the curvature of such a single step is 2 times larger than the curvature of the steps in the bunch.

IV. CONCLUSION

In an attempt to engineer the distribution of strain on the surface of a Si crystal, we used oxygen implantation in lithographically defined areas. We have examined the local strain-driven shape of steps on the Si(111) surface under the step-flow sublimation condition by AFM and *in situ* SEM. In terms of thermodynamics, the bell-like shape of the steps is interpreted as a balance between the strain-related increase of the chemical potential and the decrease of μ due to the curvature of the concave step (Gibbs-Thomson effect). On the basis of this interpretation, we derived a differential equation for the step shape and integrated this equation to reproduce the shape observed in our experiments. We also derived a simple relation [Eq. (3)] between the surface density of the strain related Gibbs free energy $\Delta G/A$ and measurable parameters like the radii of curvature R_1 and R_2 in the strained and strain-free areas. Making use of this relation, we obtained $\Delta G/A = 8.3 \times 10^{-5}$ J/m² from the shape of a step in a bunch and $\Delta G/A = 1.4 \times 10^{-4}$ J/m² from the shape of a step not belonging to a bunch.

Another conclusion concerns the strain-related bunching of steps, which takes place during the resistive heating by

both step-up and step-down electric current. The fact that bunches exist in the strained area even when the electric current has a debunching direction proves that the strain-induced attraction between the steps is a stronger driving force for bunching than the electromigration effect.

We hope that the atomic steps with their shape patterned

by localized strain on a nanoscale can act as a good template for advanced nanostructure fabrication on Si wafers.

ACKNOWLEDGMENT

This work was supported by the NEDO International Joint Research Grant Program.

*Corresponding author. FAX: +81 462 40 4718. Electronic address: homi@will.brl.ntt.co.jp

¹H.-C. Jeong and E. D. Williams, *Surf. Sci. Rep.* **34**, 171 (1999).

²T. Ogino, H. Hibino, Y. Homma, Y. Kobayashi, K. Kuniyil, K. Sumitomo, and H. Omi, *Acc. Chem. Res.* **32**, 447 (1999).

³M. B. Webb, *Surf. Sci.* **299/300**, 454 (1994).

⁴C. S. Chang, Y. M. Huang, and T. T. Tsong, *Phys. Rev. Lett.* **77**, 2021 (1996).

⁵D. E. Jone, J. P. Pelz, Y. H. Xie, P. J. Silverman, and G. H. Gilmer, *Phys. Rev. Lett.* **75**, 1570 (1995).

⁶D. E. Jones, J. P. Pelz, Y. Hong, E. Bauer, and I. S. T. Tsong, *Phys. Rev. Lett.* **77**, 330 (1996).

⁷C. M. Roland, M. G. Wensell, Y. Hong, and I. S. T. Tsong, *Phys. Rev. Lett.* **78**, 2608 (1997).

⁸J. Tersoff, Y. H. Phang, Zhenyu Zhang, and M. G. Lagally, *Phys. Rev. Lett.* **75**, 2730 (1995).

⁹F. Liu, J. Tersoff, and M. G. Lagally, *Phys. Rev. Lett.* **80**, 1268 (1998).

¹⁰H. Omi, D. J. Bottomley, and T. Ogino, *Appl. Phys. Lett.* **80**, 1073 (2002).

¹¹Y. Homma and N. Aizawa, *Phys. Rev. B* **62**, 8323 (2000).

¹²A. Pimpinelli and J. Villain, *Physics of Crystal Growth* (Cambridge University Press, Cambridge, England, 1998), Chap. 2.

¹³C. Alfonso, J. M. Bermond, J. C. Heyraud, and J. J. Métois, *Surf. Sci.* **262**, 371 (1992).

¹⁴N. C. Bartelt, J. L. Goldberg, T. L. Einstein, Ellen D. Williams, J. C. Heyraud, and J. J. Métois, *Phys. Rev. B* **48**, 15 453 (1993).

¹⁵A. V. Latyshev, H. Minoda, Y. Tanishiro, and K. Yagi, *Phys. Rev. Lett.* **76**, 94 (1996).

¹⁶D. J. Bottomley, *Jpn. J. Appl. Phys., Part 2* **36**, L1464 (1997). The sign of the Gibbs free energy under two-dimensional tensile stress in this reference is contradicted by the experimental results herein.

¹⁷J. Tersoff, C. Teichert, and M. G. Lagally, *Phys. Rev. Lett.* **76**, 1675 (1996).

¹⁸A. A. Maradudin and R. F. Wallis, *Surf. Sci.* **91**, 423 (1980).